Journal of Theoretical and Applied Vibration and Acoustics 6 (1) 81-102 (2020)

I S A V

Journal of Theoretical and Applied Vibration and Acoustics

journal homepage: http://tava.isav.ir

The influence of magnetorheological dampers on the biodynamic response of the human (pilot) body in various flight maneuvers

Heshmatolah Mohammad Khanlo [a*], **Reza Dehghani** [b]

[a] *Department of Aerospace Engineering, Shahid Sattari Aeronautical University of Science and Technology, Tehran, Iran*

[b] *Department of Mechanical Engineering, Graduate University of Advanced Technology, Kerman, Iran*

ARTICLE INFO

Article history:
Received 14 February 2020

Received in revised form
5 March 2020

Accepted 23 April 2020

Available online 18 May 2020

Keywords:

MR damper,

Transmissibility,

Biodynamic response,

Human body,

Flight maneuvers.

ABSTRACT

This paper presents the effect of a magnetorheological (MR) damper in the aircraft seat system on the body's biodynamic response for different flight maneuvers. For this purpose, discrete models 4 and 7 degrees of freedom for human modeling and the Bouc-Wen model are used to model MR damper. In various flight maneuvers, the changes in acceleration g are recorded and applied to the desired models after processing. Models used for the human body and the MR damper are compared for validation with previously published researches. The dynamic responses of the human body to these inputs without MR dampers and with an MR damper are investigated. The transmissibility[†] of the seat to the human body is used as a parameter that is common in these types of analyses. The results show that the use of MR dampers has a significant effect on reducing the transmissibility in maneuvers with a sudden increase in acceleration and also significant changes in the frequency at which maximum transmissibility is achieved.

1. Introduction

The body vibration and biodynamic behavior of the human (pilot) are some significant areas in designing the aircraft seat system. The field studies show that pilots complain of a series of physical discomfort. These include pain in the neck and spine, and so on. On the other hand,

* Corresponding author:
E-mail address: khanloh47@yahoo.com (H. M. Khanlo)

http://dx.doi.org/10.22064/tava.2021.105238.1132

increasing demand for training and operational flights and the duration of the flight can aggravate the problem. Studies have also shown that such discomfort can cause inattention with loss of situational awareness and poor decision making in both training and missions [1, 2].

Over the past two decades, many researchers have been working on new ways to reduce seat vibration by controlling stiffness and damping. In this regard, the use of electrorheological (ER) and magnetorheological (MR) damper is one of the methods of semi-active or active control to reduce vibrations[3, 4]. However, due to fast response time, continuous control of damping, simple design, adaptability to high-temperature variations, high damping force, low power consumption, and inherent stability of the system, MR dampers are preferred to ER damper [5, 6].

Many studies have been done on the use of MR dampers with a variety of applications in ground vehicles. Carlson [7] used three examples of the use of MR dampers in a heavy-duty car seat, seismic system, and a washing machineshowing that in all cases, the range of harmful vibration greatly reduces. Orecny *et al*. [8] studied the application of an MR damper and a dynamic absorber for a suspension of a working machine seat. They showed that the effect of a dynamic absorber in the presence of a magnetic damper is negligible, while it alone has a significant effect on reducing the amplitude of vibration. Choi *et al*. [9] studied the vibration control of an MR seat damper for commercial vehicles. They showed the effectiveness of MR damper to isolate the vibration through hard-ware-in-the loop simulation. In addition, they showed the effectiveness of MR damper by reducing the vibration levels at the driver's seat under both bump and random road profiles.

Several studies have also been conducted to reduce vibrations in the helicopter seat and airplane seat. Choi *et al*.[10] studied the reduction of biodynamic responses to shock loads using MR helicopter crew seat suspensions. They analyzed the vibration of the seat system with sinusoidal and shock inputs. The results showed that for the sinusoidal excitation case, the semi-active MR seat system has better vibration attenuation performance over the simulated frequency range than both the passive hydraulic or passive MR seat suspensions. It has also been shown that for the shock load case, both the passive and semi-active MR seat suspensions present better shock reduction performance than the passive hydraulic seat suspension. Heimens *et al*. [11] investigated the suspension system of helicopter crew seats with a semi-active MR damper to enhance occupant comfort and reduce health issues resulting from body vibration. Their experimental results showed that the transmitted induced vertical vibration can be reduced to 61-70%, depending on the type of seat cushion, by MR damper. This study also showed that, although the dynamics of a tactical vehicle seat may be complex, a single degree freedom model can be a valuable tool for MR damper design and performance predictions.

A review of past researches has shown that there is a relatively large amount of work on the use of magnetic damper on ground vehicles, but there is not much research in aerial vehicles, especially in aircraft. Also, in previous studies, the system input was typically either sinusoidal or shock-induced form. Using an MR damper with real inputs from various flight maneuvers in the pilot's seat and investigate its effect on the system response are the main contributions of this paper. The rest of this paper is organized as: in Section 2, the modeling techniques of the pilot body on the seat are presented. In Section 3, the flight maneuvers are introduced and simulated. The final section is dedicated to summarizing the results and conclusions.

2. Mathematical modeling

In this section, the mathematical modeling of the system is derived. There has been a lot of research in this field. The models can be categorized into three main groups: continuum, discrete, and lumped parameter models [12, 13]. In continuum models, the human spine is modeled as a single flexible beam. Matsumoto and Griffin [14] have done considerable works in this area and have shown that finite element based models can accurately capture the motion of the spine's response to vertical accelerations. This approach was adopted by Wood *et al*.[15], which used beam theory to model arm dynamics. On the other hand, in the discrete models, the spine is considered as rigid bodies connected by springs and dampers. The response of this multi-body system may be obtained by solving the differe ntial equations of the motion. Both the continuous and discrete systems have their characteristics and complexity. The discrete system seeks to establish the fact that each body member has its particular frequency resonance [13-16]. Lumped parameter models try to find the dynamic response of the body using an equivalent mass–spring–damper system. Although the models of this type usually have one or two degrees of freedom, they are quite useful in analyzing the response to the vertical base excitation [17]. However, Sirouspour *et al* [18] showed that this method has some difficulties in modeling the transverse vibration of the human body.

Here, the lumped parameter model is used. In this type of modeling, models with different degrees of freedom are presented. For example, we can refer to the 4 DOF [19] and the 7 DOF [20] that are commonly-used models. Because in this article, a magnetic damper has been added between the body of the aircraft and its seat, we are introducing the magnetic damper before the extraction of the equations of motion for each model. In the case of MR damper, a lot of research has been done and several models have been presented [21-23]. Among the modeling methods, parametric models appear to be a simple and reliable method for obtaining a mathematical model of physical MR damper [22]. There are several numerical models for predicting the magnetic damper response. These models include Bingham, bi-viscous, visco-elastic-plastic, Hydro-mechanical, Maxwell, Bouc-Wen, Dahl, LuGre, hyperbolic tangent, sigmoid, equivalent, and phase transition. Among these, Bingham and Bouc-Wen models are the most commonly used models to predict the behavior of MR dampers.

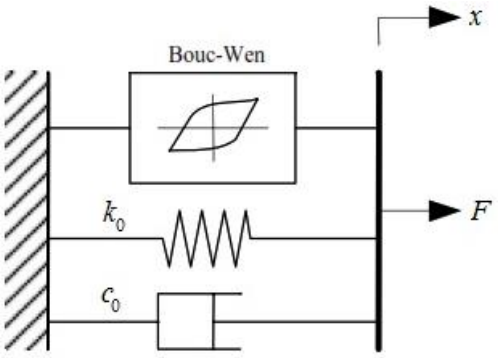

Fig. 1 Bouc-Wen MR damper model.

In this research, the Bouc-Wen MR damper model is used. A simple Bouc-Wen model, as shown in Fig. 1, consists of three parts: spring, damper, and Bouc-Wen block. According to the configuration shown in Fig. 1, the damping force is as follows [22]:

$$F(t) = c_0\dot{x} + k_0(x - x_0) + \alpha z \tag{1}$$

where c_0 is the viscous damping coefficient, k_0 the stiffness coefficient, x_0 is used to account for the effect of the accumulator as $f_0 = k_0 x_0$ and z is an evolutionary variable associated with the Bouc-Wen block that given by:

$$\dot{z} = -\gamma|\dot{x}|z|z|^{n-1} - \beta\dot{x}|z|^n + A_0\dot{x} \tag{2}$$

Parameters c_0, k_0, α, β, γ, n and A_0 commonly referred to as characteristic or shapes parameters of the Bouc–Wen model in MR dampers, that are functions of the electrical current, amplitude, and frequency of excitation. However, experimental tests performed in Ref. [22] show that the parameters A_0, β, γ, and k_0 have little variation with frequency, amplitude and current. But with the change of current, the changes of the parameters α and c_0 are significant. In the next section, the numerical simulation of each of the above models is discussed.

Figure 2 shows the pilot's biochemical model. In the following, the equations of motion are derived for each of these models. These equations are obtained by using Newton's law on the model. Hence, the differential equations of human body motion with Wan's model are given as follows:

$$m_1\ddot{x}_1 + c_1(\dot{x}_1 - \dot{x}_2) + k_1(x_1 - x_2) = 0 \tag{3}$$

$$m_2\ddot{x}_2 - c_1(\dot{x}_1 - \dot{x}_2) - k_1(x_1 - x_2) + c_2(\dot{x}_2 - \dot{x}_3) + k_2(x_2 - x_3) + c_3(\dot{x}_2 - \dot{x}_4) + k_3(x_2 - x_4) = 0 \tag{4}$$

$$m_3\ddot{x}_3 - c_2(\dot{x}_2 - \dot{x}_3) - k_2(x_2 - x_3) + c_4(\dot{x}_3 - \dot{x}_4) + k_4(x_3 - x_4) = 0 \tag{5}$$

$$m_4\ddot{x}_4 - c_4(\dot{x}_3 - \dot{x}_4) - k_4(x_3 - x_4) - c_3(\dot{x}_2 - \dot{x}_4) - k_3(x_2 - x_4) + c_5(\dot{x}_4 - \dot{x}_5) + k_5(x_4 - x_5) = 0 \tag{6}$$

$$m_5\ddot{x}_5 - c_5(\dot{x}_4 - \dot{x}_5) - k_5(x_4 - x_5) + k_6(x_5 - x_{in}) + F_{MR} = 0 \tag{7}$$

Where, in Eq. (7), x_{in} and F_{MR} are the input displacement and MR damper force to the seat base, respectively. It should be noted that F_{MR} is obtained by replacing the x and $\dot{x}$ by $x_5 - x_{in}$ and $\dot{x}_5 - \dot{x}_{in}$, respectively in equations (1) and (2) for current Wan's model. In this model, the head and neck with mass m_1, stiffness k_1 and damping c_1, the upper torso with mass m_2, stiffness k_2 and damping c_2, the lower torso with mass m_3, stiffness k_3 and damping c_3 and the pelvic with mass m_4, stiffness k_4 and damping c_4 are connected to each other.

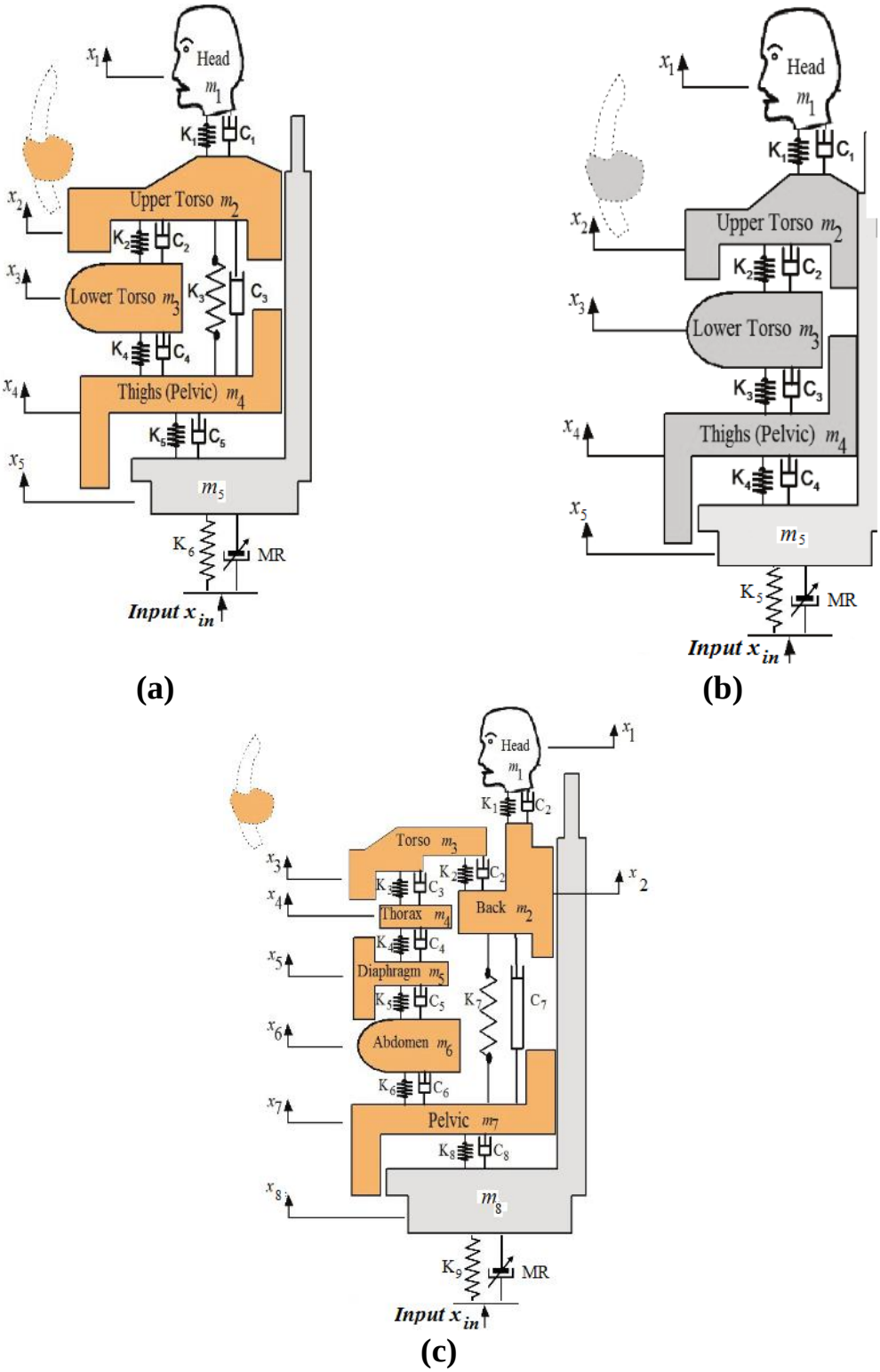

Fig. 2 Biomechanical models of the pilot: (a) Wan and Schimmels 4-DOF model with MR damper, (b) 4-DOF Boileau and Rakheja model with MR damper, (c) Patil and Palanichamy 7-DOF model with MR damper [20].

The differential equations of human body motion with Boileau's model can be obtained as follows:

$$m_1\ddot{x}_1 + c_1(\dot{x}_1 - \dot{x}_2) + k_1(x_1 - x_2) = 0 \tag{8}$$

$$m_2\ddot{x}_2 - c_1(\dot{x}_1 - \dot{x}_2) - k_1(x_1 - x_2) + c_2(\dot{x}_2 - \dot{x}_3) + k_2(x_2 - x_3) = 0 \tag{9}$$

$$m_3\ddot{x}_3 - c_2(\dot{x}_2 - \dot{x}_3) - k_2(x_2 - x_3) + c_3(\dot{x}_3 - \dot{x}_4) + k_3(x_3 - x_4) = 0 \tag{10}$$

$$m_4\ddot{x}_4 - c_3(\dot{x}_3 - \dot{x}_4) - k_3(x_3 - x_4) + c_4(\dot{x}_4 - \dot{x}_5) + k_4(x_4 - x_5) = 0 \tag{11}$$

$$m_5\ddot{x}_5 - c_4(\dot{x}_4 - \dot{x}_5) - k_4(x_4 - x_5) + k_5(x_5 - x_{in}) + F_{MR} = 0 \tag{12}$$

Also, in this case, F_{MR} is obtained by replacing the x and $\dot{x}$ by $x_5 - x_{in}$ and $\dot{x}_5 - \dot{x}_{in}$, respectively in equations (1) and (2) for current Boileau's model.

And the differential equations of human body motion with Patil's model are given as follows:

$$m_1\ddot{x}_1 + c_1(\dot{x}_1 - \dot{x}_2) + k_1(x_1 - x_2) = 0 \tag{13}$$

$$m_2\ddot{x}_2 - c_1(\dot{x}_1 - \dot{x}_2) - k_1(x_1 - x_2) + c_2(\dot{x}_2 - \dot{x}_3) + k_2(x_2 - x_3) + c_7(\dot{x}_2 - \dot{x}_7) + k_7(x_2 - x_7) = 0 \tag{14}$$

$$m_3\ddot{x}_3 - c_2(\dot{x}_2 - \dot{x}_3) - k_2(x_2 - x_3) + c_3(\dot{x}_3 - \dot{x}_4) + k_3(x_3 - x_4) = 0 \tag{15}$$

$$m_4\ddot{x}_4 - c_4(\dot{x}_4 - \dot{x}_5) - k_4(x_4 - x_5) - c_3(\dot{x}_3 - \dot{x}_4) - k_3(x_3 - x_4) = 0 \tag{16}$$

$$m_5\ddot{x}_5 - c_4(\dot{x}_4 - \dot{x}_5) - k_4(x_4 - x_5) - c_5(\dot{x}_5 - \dot{x}_6) - k_5(x_5 - x_6) = 0 \tag{17}$$

$$m_6\ddot{x}_6 - c_5(\dot{x}_5 - \dot{x}_6) - k_5(x_5 - x_6) + c_6(\dot{x}_6 - \dot{x}_7) + k_6(x_6 - x_7) = 0 \tag{18}$$

$$m_7\ddot{x}_7 - c_6(\dot{x}_6 - \dot{x}_7) - k_6(x_6 - x_7) - c_7(\dot{x}_2 - \dot{x}_7) - k_7(x_2 - x_7) + c_8(\dot{x}_7 - \dot{x}_8) + k_8(x_7 - x_8) = 0 \tag{19}$$

$$m_8\ddot{x}_8 - c_8(\dot{x}_7 - \dot{x}_8) - k_8(x_7 - x_8) + k_9(x_8 - x_{in}) + F_{MR} = 0 \tag{20}$$

In this model, the head and neck with mass m_1, stiffness k_1 and damping c_1, the shoulder back with mass m_2, stiffness k_2 and damping c_2, the torso with mass m_3, stiffness k_3 and damping c_3, the thorax with mass m_4, stiffness k_4 and damping c_4, the diaphragm with mass m_5, stiffness k_5 and damping c_5, the abdomen with mass m_6, stiffness k_6 and damping c_6 and the pelvis with mass m_7, stiffness k_8 and damping c_8 are connected to each other. Also, stiffness k_7 and damping c_7 are considered between the shoulder back and the pelvis. Also, F_{MR} is obtained by replacing the x and $\dot{x}$ by $x_8 - x_{in}$ and $\dot{x}_8 - \dot{x}_{in}$, respectively in equations (1) and (2) for the current Patil's model.

3 . Numerical simulation results

In this section, at first, the method of recording experimental data during flight and in various maneuvers is presented, and then numerical simulation of each model using MATLAB software and the analysis of output from them are discussed. In the program written in MATLAB

software, they are first integrated from the acceleration recorded by the data recording device, and these are applied to different body models in the form of base displacement or input excitation; then, by taking FFT, the transmissibility (in the ratio of output to input) is plotted as frequency response.

3.1.Different flight maneuvers

The data recorder is shown in Fig.3, which comprises the main unit, communication cables, and an active receiving antenna. The device used here is equipped with a powerful processor with 8 input channels and up to 16 channels of output, as well as a recording capability of up to 18 g and an input voltage of 5.6 to 15 V with a current of 550 mA at 8 V, and it is capable to record data with frequency up to 100 Hz. This device has digital capabilities to show actual aircraft speed, engine speed, or engine temperature, and so on, but because the above information is not required, this is not done and only the information about the changes in g has been recorded in various maneuvers. This device is connected under the seat and exactly on the floor of the aircraft cabin.

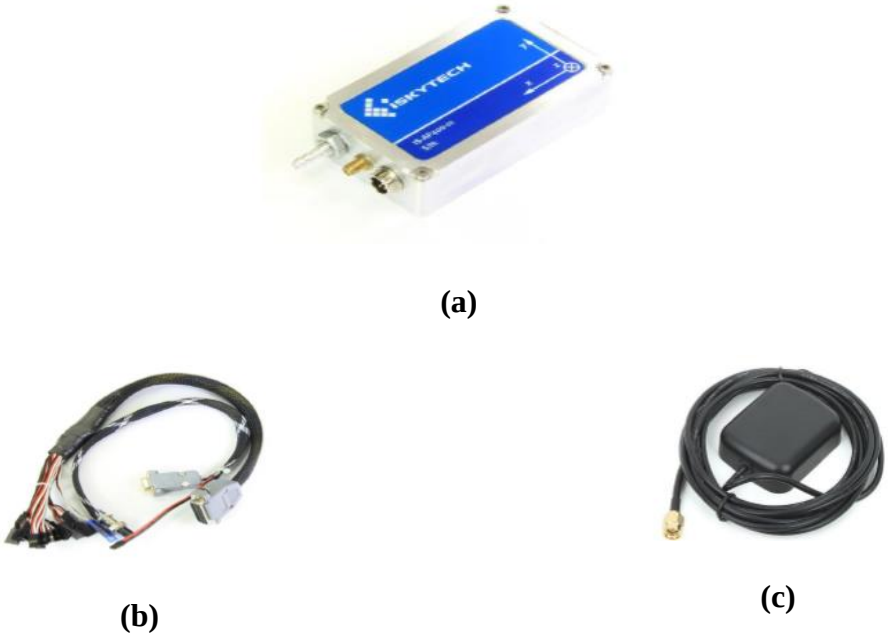

Fig. 3 Data recorder: (a) main unit, (b) communication cables, (c) active receiver antenna.

In this research, seven different flight maneuvers have been conducted as follows: lazy eight maneuvers (maneuver 1), Barrel roll maneuver (maneuver 2), Immelman maneuver (maneuver 3), Cuban eight maneuver (maneuver 4), loop maneuver (maneuver 5), split S maneuver (maneuver 6), chandelle maneuver (maneuver 7). More details on maneuvers have presented in [24][24].

Figure 4 shows the acceleration g recorded in different flight maneuvers. These accelerations are applied as inputs to each of the models in question in order to investigate the biodynamic behavior of the pilot's body.

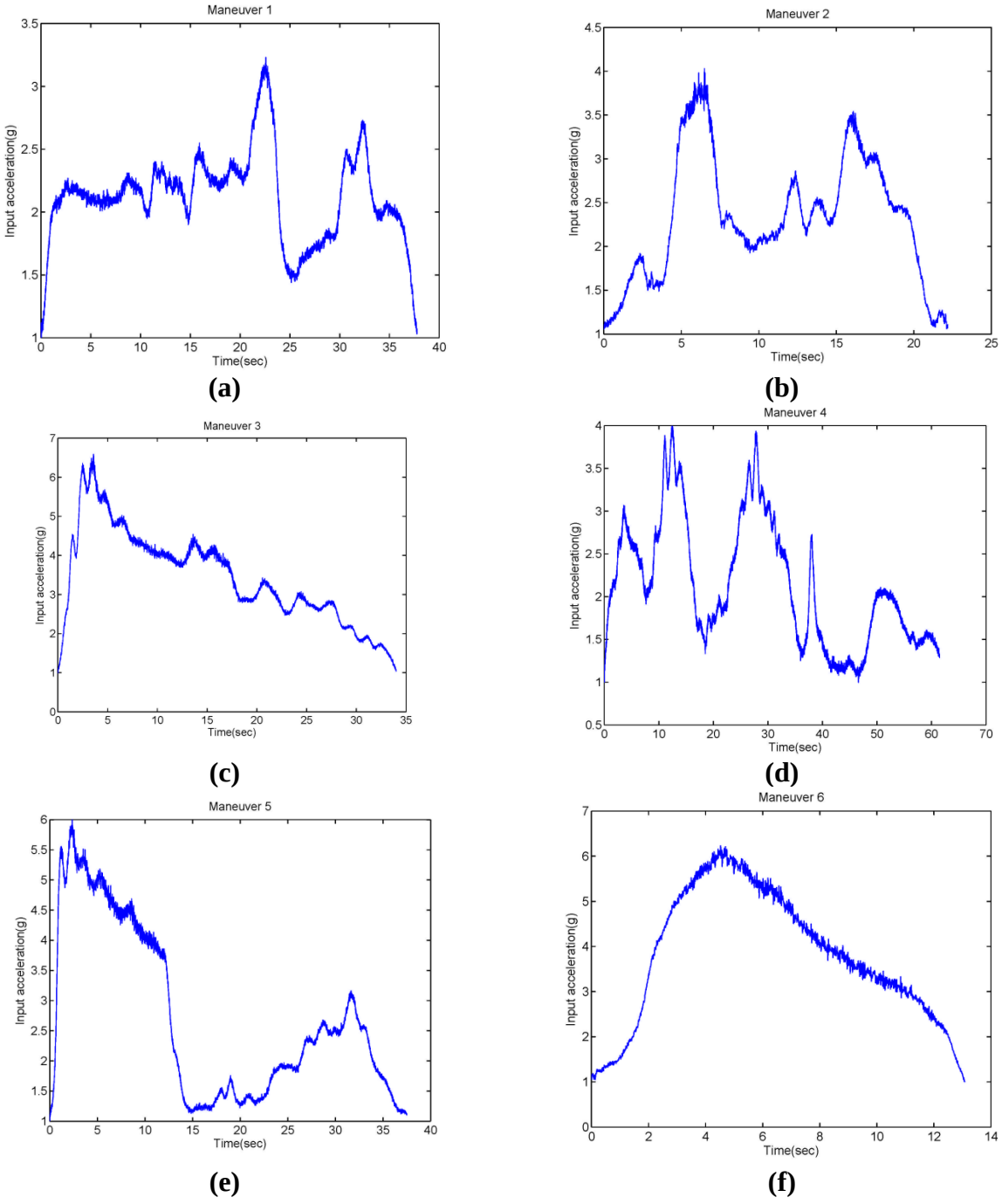

Fig. 4 Actual input accelerations in different flight maneuvers: (a) Lazy eight, (b) Barrel roll, (c) Immelmann, (d) Cuban eight, (e) Loop, (f) Split S, (g) Chandelle.

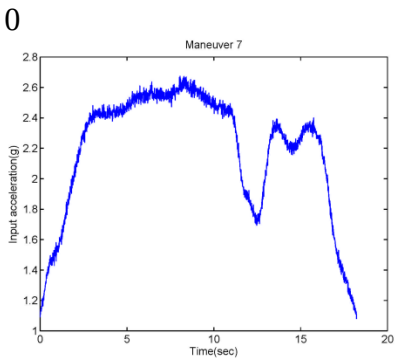

Fig. 4 Actual input accelerations in different flight maneuvers: (a) Lazy eight, (b) Barrel roll, (c) Immelmann, (d) Cuban eight, (e) Loop, (f) Split S, (g) Chandelle.

Since the magnetic damper has been added to these models, its verification is done first. In the Bouc-Wen MR damper model, according to equations (1) and (2), a number of coefficients are constant and some are also dependent on the electrical current. It is assumed that $n=2$ and the force offset $f_0=40\,N$ has the same value as the Bingham model force offset since the accumulator produces a nearly constant force offset. The average values of the other current independent parameters are $A_0=30.852$, $\beta=0.081\,mm^{-2}$, $\gamma=1.507\,mm^{-2}$ and $k_0=1.984\,N/mm$. The current dependent parameters are given as follows [22]:

$$\alpha(I)=-305.60I^3+377.83I^2+103.87I+11.76 \tag{21}$$

$$c_0(I)=-3.20I^3-3.77I^2+15.37I+0.85 \tag{22}$$

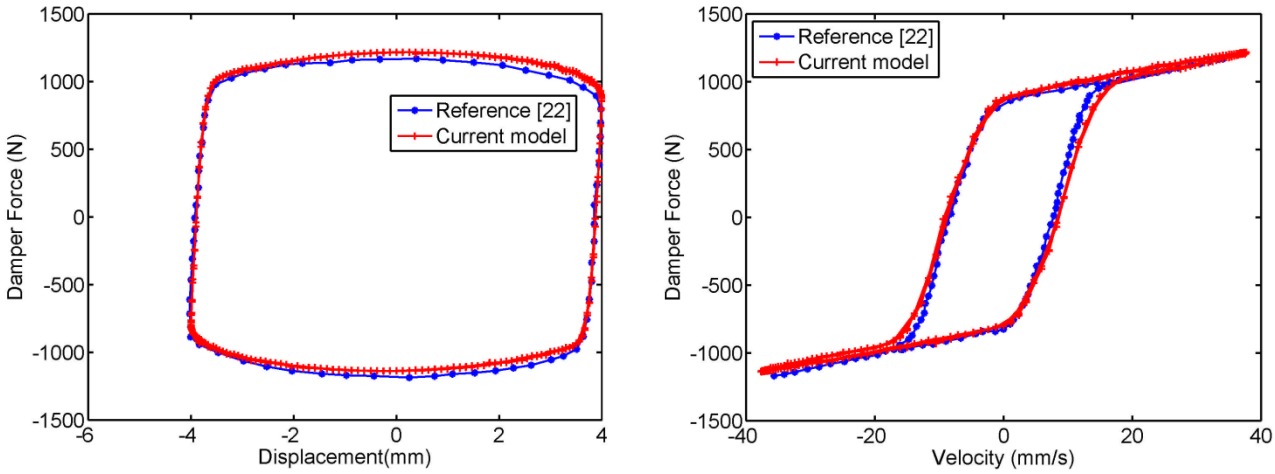

Fig. 5 Bouc-Wen MR damper verification (F=1.50 Hz, Amp=4 mm and I=1 A).

Figure 5 shows the results of the MR damper force with the Bouc-Wen model in terms of displacement and speed is driven by harmonic excitation with frequency $1.5\,Hz$ with amplitude $4\,mm$ and an operating current of $I=1\,A$. As shown, there is a good agreement between the results of the reference [22] and the current research.

In the following, the acceleration of aircraft in each maneuver is introduced as inputs to the models mentioned here. Then, the biodynamic response of each body organ is examined. Of course, before performing numerical simulations for each of the models, their validation is done.

3.2.Biodynamic responses with Wan model

Wan's model combines a body with four lumped masses: the head, upper torso, lower torso and pelvic with a spring and a damper. Also, in this model, the upper torso is connected by a spring, and damper to the pelvic. At first, validation of the model is done by comparing the results of the current research with reference [20]. The input required for verification is a harmonic displacement with a unique amplitude. Seat-to-head transmissibility is considered as a response to the input. The numerical values of the parameters for this model are given in Table 1.

Table 1 Biomechanical parameters of the Wan model [20].

Body member	Parameter	Values
Head	m_1	4.17 (kg)
	k_1	134400 (N/m)
	c_1	250 (N.s/m)
Upper torso	m_2	15(kg)
	k_2	10000 (N/m)
	c_2	200 (N.s/m)
Lower torso	m_3	5.5(kg)
	k_3	192000 (N/m)
	c_3	900.1(N.s/m)
Pelvic	m_4	36(kg)
	k_4	20000 (N/m)
	c_4	300(N.s/m)
	k_5	49340 (N/m)
	c_5	2475(N.s/m)
Seat	m_5	30(kg)
	k_6	19325 (N/m)

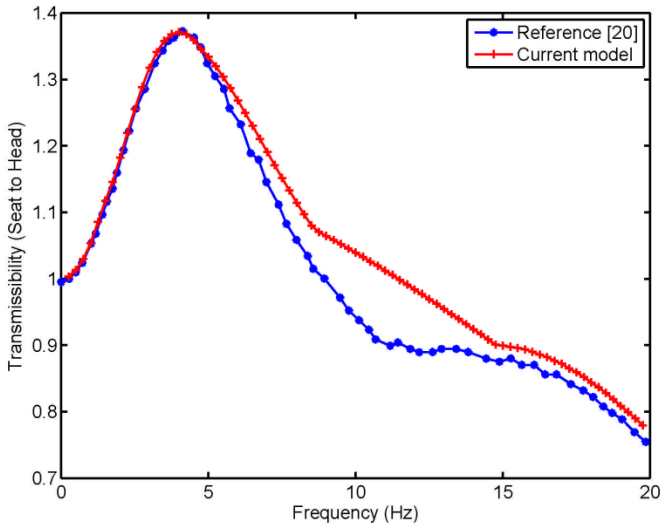

Fig. 6 Compare the current Wan model with reference [20].

Table 2 Maximum transmissibility and corresponding frequency for Wan and Schimmels 4-DOF model.

Maneuvers No.		1		2		3		4		5		6		7	
Section		TR	F (Hz)	TR	F (Hz)	TR	F (Hz)	TR	F (Hz)	TR	F (Hz)	TR	F (Hz)	TR	F (Hz)
Head	Without MR	2.08	0.56	2.73	1.49	3.1	0.59	1.87	0.5	4.42	0.67	2.62	1.53	2.2	1.43
	With MR	0.56	1.83	1.01	1.76	0.24	1.89	0.35	1.84	0.17	1.87	1.05	1.99	0.85	1.92
Upper Torso	Without MR	2.07	0.56	2.71	1.49	3.1	0.59	1.86	0.5	4.41	0.67	2.61	1.53	2.18	1.43
	With MR	0.55	1.83	1.0	1.76	0.24	1.89	0.35	1.84	0.17	1.87	1.04	1.99	0.84	1.92
Lower Torso	Without MR	2.09	0.56	2.77	1.49	3.11	0.59	1.88	0.5	4.45	0.67	2.65	1.53	2.23	1.43
	With MR	0.57	1.83	1.03	1.76	0.25	1.89	0.36	1.84	0.18	1.87	1.07	1.99	0.86	1.92
Pelvic	Without MR	2.05	0.56	2.67	1.49	3.08	0.59	1.85	0.5	4.36	0.67	2.56	1.53	2.14	1.43
	With MR	0.53	1.83	0.97	1.76	0.23	1.89	0.33	1.84	0.17	1.87	1.07	1.99	0.81	1.92

As shown in Figure 6, there is good agreement between the results. There are some differences between the two results in some frequency ranges that can be due to the lack of knowledge of the type of solver and the program used or the step sizes. However, since the frequency band at which the maximum transmissibility occurs is below this range, there should be no particular concern. It is important to note that the biodynamic response of the seated human body subject to complete vibration is divided into two categories. The first category "To-the-body" force motion interrelation as a function of frequency at the human-seat interface, expressed as the driving-point mechanical impedance or the apparent mass. The second category "Through-the-body" response function, generally termed as seat-to-head transmissibility for the seated occupant [20]. Seat-to-head transmissibility is defined as the ratio of output responses (head) to input excitation. Here, with MR dampers, the input excitation is applied to the base of the damper assembly in the form of a base displacement, and the transmissibility is used as the ratio of the output-to-input responses. It is important to note that for the case without MR damper, the displacement excitation is applied directly to the seat. Transmissibility for other body members is also calculated, and the results are presented in Table 2.

The results of Table 2 show that in all maneuvers, the use of an MR damper has a significant effect on reducing the transmissibility of the seat to any of the body organs. The use of an MR damper affects the system's dynamics and results in maximum transmissibility at a higher frequency. The results of this model show that in maneuvers 5, 3, and 4, the MR damper exhibits the greatest reduction in transmissibility. However, as shown in Figure 4, these maneuvers had a sudden increase in acceleration and significant transmissibility to the body. So it can be said that these types of dampers are more effective in sudden acceleration. Depending on how the body organs connect and how close their frequencies are to each other, the transmissibility of the different organs does not change significantly. Maximum transmissibility also occurs at the first frequency, so no change in frequencies is observed.

To confirm the results obtained in Table 2, for example, we select maneuver 1 and the biodynamic response of body organs to the input from this maneuver is shown in Fig. 7. The results confirm the values of Table 2 in the relevant maneuver and also show the effectiveness of the MR damper on the response of the pilot's body.

3.3.Biodynamic responses with Boileau model

This model is similar to Wan's model exception that the springs and damper between the upper torso and pelvic are eliminated in this model. As in the previous model, this model is validated first. Then, the input from different maneuvers is applied to the model. The numerical values of the parameters for this model are given in Table 3.

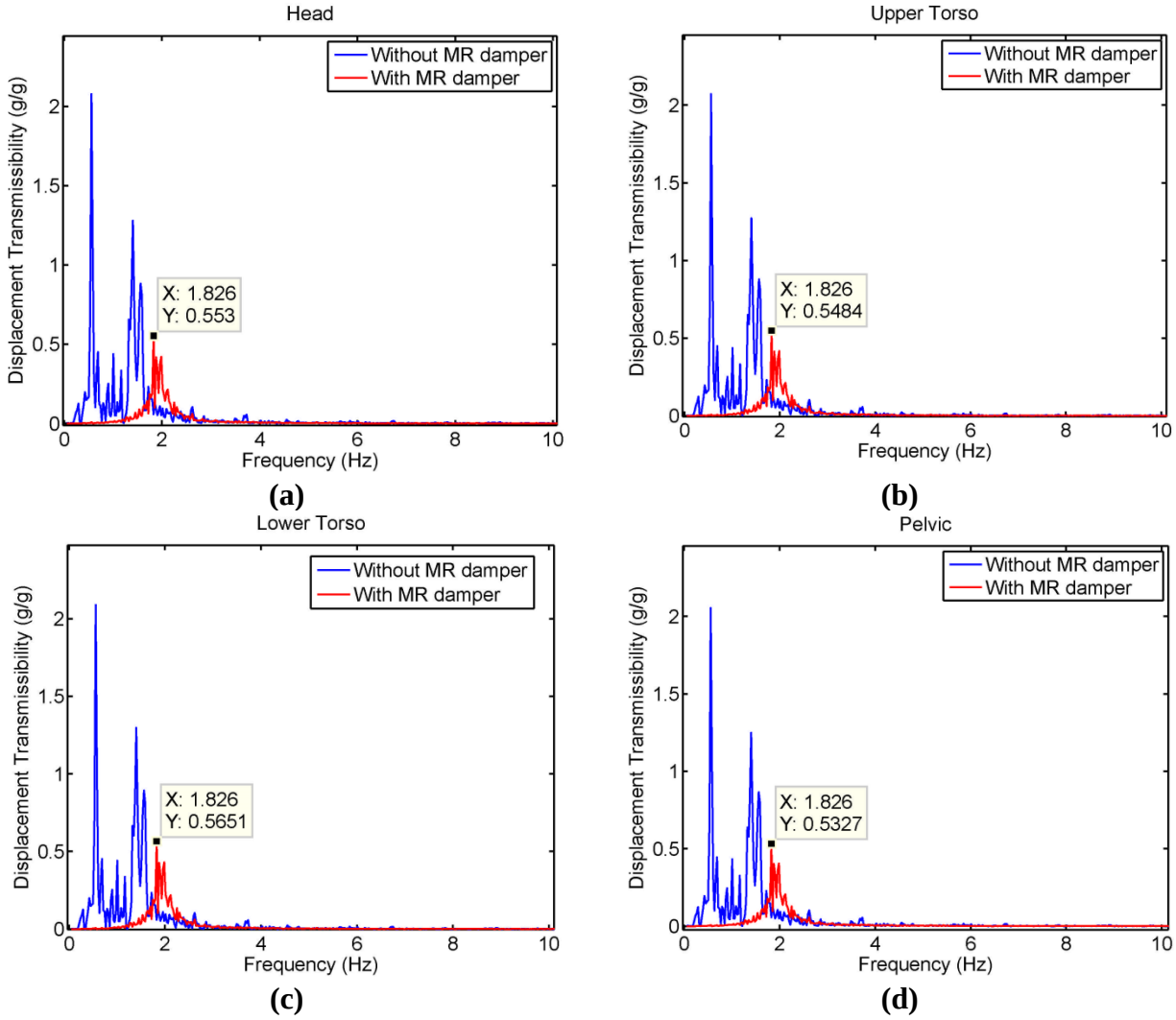

Fig. 7 Typical biodynamic responses of the human body with Wan model in maneuver 1: (a) head section, (b) upper torso section, (c) Lower torso section, (d) pelvic section.

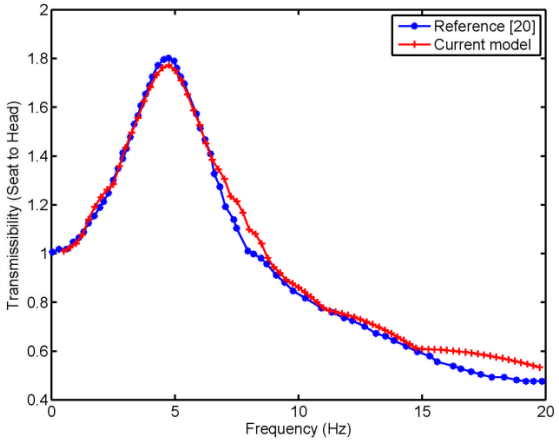

Fig. 8 Compare the current Boileau model with reference [20].

Table 3 Biomechanical parameters of the Boileau model [20].

Body member	Parameter	Values
Head	m_1	5.31 (kg)
	k_1	310000 (N/m)
	c_1	400 (N.s/m)
Upper torso	m_2	28.49(kg)
	k_2	183000 (N/m)
	c_2	4750 (N.s/m)
Lower torso	m_3	8.62(kg)
	k_3	162800 (N/m)
	c_3	4585(N.s/m)
Pelvic	m_4	12.78(kg)
	k_4	90000 (N/m)
	c_4	2064(N.s/m)
Seat	m_5	30(kg)
	k_5	19325 (N/m)

Figure 8 shows the comparison result of the current model and the reference [20]. As it can be seen, there is a good match between the two models. In this model, the transmissibility of the input excitation to all body organs is given in Table 4.

Generally, in this model, the MR damper also reduces the transmissibility of most maneuvers. The results of this model show that in maneuvers 5, 4, and 3, the MR damper exhibits the greatest reduction in transmissibility. However, in maneuvers 2 and 7, the MR damper partly increased the transmissibility of the body organs of the pilot. In this case, the use of a magnetic damper also leads to an increase in the frequency of maximum transmissibility. These results show that MR dampers have little or no effect on gradual acceleration.

To confirm the results of Table 4, maneuver 1 is selected and the biodynamic response of the pilot organs is shown in Fig. 9.

Table 4 Maximum transmissibility and corresponding frequency for Boileau and Rakheja 4-DOF model.

Maneuvers No.		1		2		3		4		5		6		7	
Section		TR	F (Hz)	TR	F (Hz)	TR	F (Hz)	TR	F (Hz)	TR	F (Hz)	TR	F (Hz)	TR	F (Hz)
Head	Without MR	0.82	0.56	0.87	1.76	1.93	0.62	2.4	0.57	2.6	0.67	1.07	1.84	0.5	1.87
	With MR	0.61	1.98	0.97	2.07	0.21	1.97	0.41	2.05	0.23	1.95	0.99	1.99	0.69	2.09
Upper Torso	Without MR	0.82	0.56	0.87	1.76	1.93	0.62	2.4	0.57	2.6	0.67	1.06	1.84	0.5	1.87
	With MR	0.61	1.98	0.96	2.07	0.21	1.97	0.4	2.05	0.23	1.95	0.99	1.99	0.68	2.09
Lower Torso	Without MR	0.81	0.56	0.84	1.76	1.92	0.62	2.36	0.57	2.54	0.67	1.02	1.84	0.48	1.87
	With MR	0.57	1.98	0.91	2.07	0.2	1.97	0.38	2.05	0.22	1.95	0.94	1.99	0.65	2.09
Pelvic	Without MR	0.79	0.56	0.79	1.76	1.92	0.62	2.32	0.57	2.46	0.67	0.96	1.84	0.45	1.87
	With MR	0.53	1.98	0.84	2.07	0.19	1.97	0.35	2.05	0.21	1.95	0.87	1.99	0.6	2.09

3.4.Biodynamic responses with Patil model

This model is 7 degrees of freedom so that the human body is shown in greater detail, which allows the dynamical behavior to be examined more comprehensively. Like previous models, system validation is done by comparing the current research with reference [20]. The numerical values of the parameters for this model are given in Table 5.

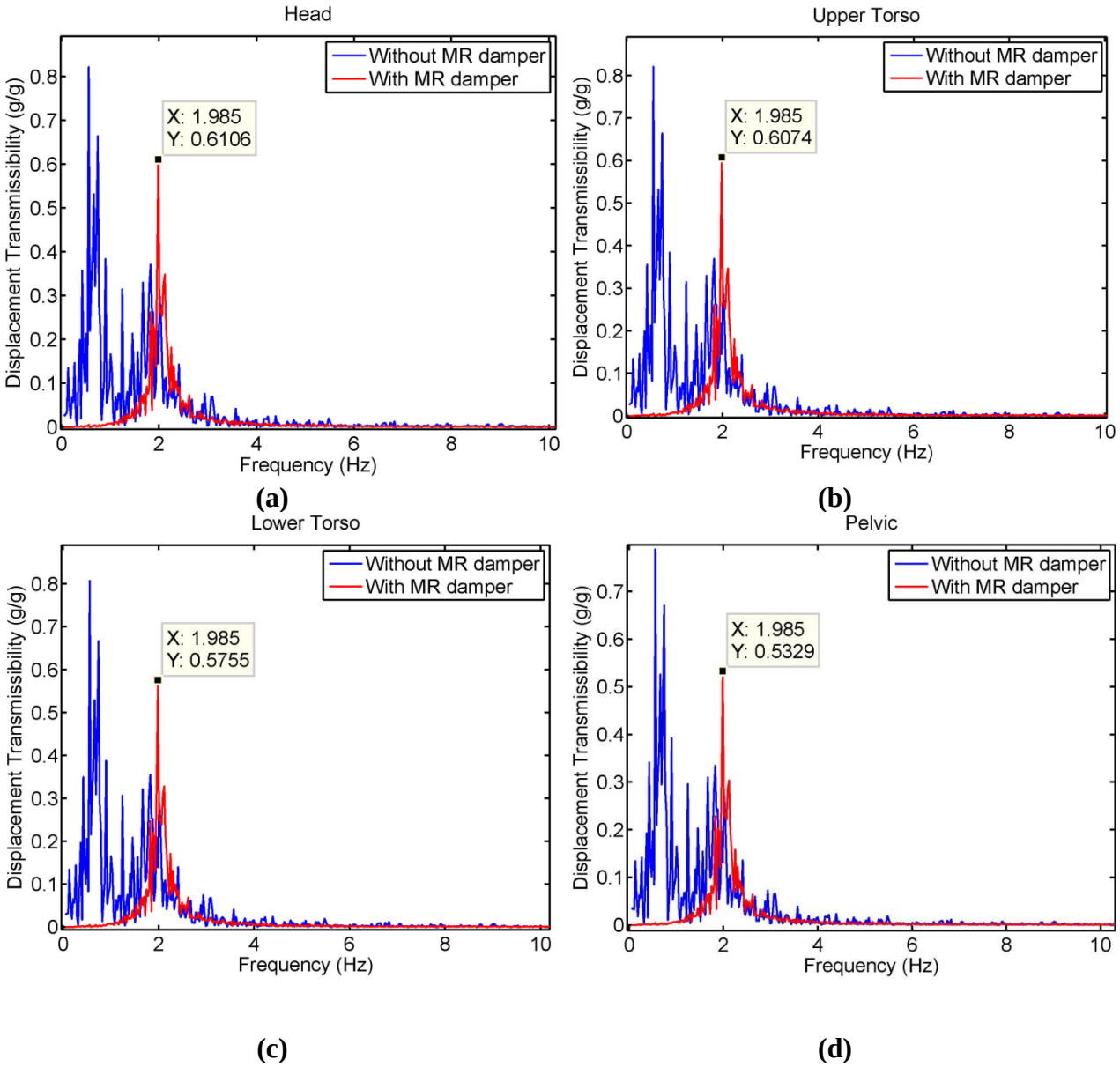

Fig. 9 Typical biodynamic responses of the human body with Boileau model in maneuver 1: (a) head section, (b) upper torso section, (c) Lower torso section, (d) pelvic section.

Table 5 Biomechanical parameters of the Patil model [20].

Body member	Parameter	Values
Head	m_1	5.55 (kg)
	k_1	53640 (N/m)
	c_1	3561 (N.s/m)
Back	m_2	6.94(kg)
	k_2	53640 (N/m)
	c_2	3651 (N.s/m)
Torso	m_3	33.33 (kg)
	k_3	8941 (N/m)
	c_3	298(N.s/m)
Thorax	m_4	1.389 (kg)
	k_4	845 (N/m)
	c_4	298 (N.s/m)
Diaphragm	m_5	0.4629 (kg)
	k_5	8941 (N/m)
	c_5	298 (N.s/m)
Abdomen	m_6	6.02 (kg)
	k_6	8941 (N/m)
	c_6	298 (N.s/m)
Pelvis	m_7	27.7 (kg)
	k_7	53640 (N/m)
	c_7	3651 (N.s/m)
	k_8	25500 (N/m)
	c_8	378 (N.s/m)
Seat	m_8	30(kg)
	k_9	19325 (N/m)

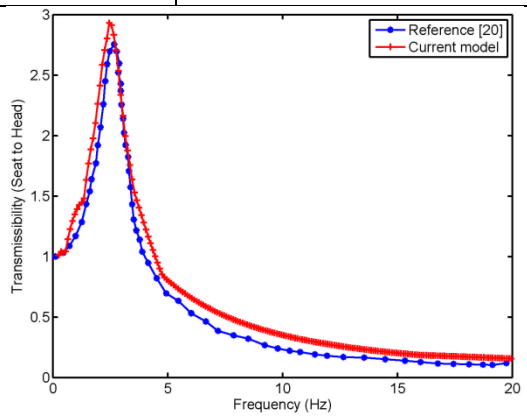

Fig. 10 Compare the current Patil model with reference [20].

Figure 10 shows the result of the validation of the current model in comparison with the reference [20]. As it can be seen, there is a good match between the two models. With this model, the transmissibility of the input excitation to all body organs is given in Table 6.

Table 6 Maximum transmissibility and corresponding frequency for Patil and Palanichamy 7-DOF model.

Maneuvers No.		1		2		3		4		5		6		7	
Section		TR	F (Hz)	TR	F (Hz)	TR	F (Hz)	TR	F (Hz)	TR	F (Hz)	TR	F (Hz)	TR	F (Hz)
Head	Without MR	1.89	0.56	0.95	1.44	1.77	0.62	4.09	0.42	3.85	0.4	1.31	1.61	0.99	1.54
	With MR	0.5	1.53	1.24	1.58	0.5	1.59	0.52	1.56	0.25	1.6	1.0	1.61	0.71	1.54
Back	Without MR	1.88	0.56	0.94	1.44	1.77	0.62	4.08	0.42	3.84	0.4	1.29	1.61	0.98	1.54
	With MR	1.22	0.93	1.22	1.58	0.49	1.59	0.52	1.56	0.24	1.6	0.98	1.61	0.7	1.54
Torso	Without MR	1.98	0.56	1.04	1.44	1.78	0.62	4.18	0.42	3.95	0.4	1.46	1.61	1.07	1.54
	With MR	0.55	1.53	1.38	1.58	0.55	1.59	0.58	1.56	0.27	1.6	1.11	1.61	0.79	1.54
Thorax	Without MR	2.0	0.56	0.83	1.44	1.74	0.62	4.15	0.42	3.91	0.4	1.5	1.61	1.07	1.54
	With MR	0.56	1.53	1.4	1.58	0.56	1.59	0.59	1.56	0.28	1.6	1.12	1.61	0.8	1.54
Diaphragm	Without MR	2.0	0.56	1.03	1.44	1.72	0.62	4.12	0.42	3.87	0.4	1.48	1.61	1.05	1.54
	With MR	0.55	1.53	1.38	1.58	0.55	1.59	0.58	1.56	0.27	1.6	1.11	1.61	0.79	1.54
Abdomen	Without MR	1.98	0.56	0.81	1.44	1.79	0.62	4.09	0.42	3.83	0.4	1.46	1.61	1.03	1.54
	With MR	0.54	1.53	1.35	1.58	0.54	1.59	0.57	1.56	0.27	1.6	1.09	1.61	0.78	1.54
Pelvic	Without MR	1.75	0.56	0.81	1.44	1.77	0.62	3.94	0.42	3.7	0.4	1.08	1.61	0.87	1.54
	With MR	0.41	1.53	1.04	1.58	0.42	1.59	0.44	1.56	0.21	1.6	0.83	1.61	0.59	1.54

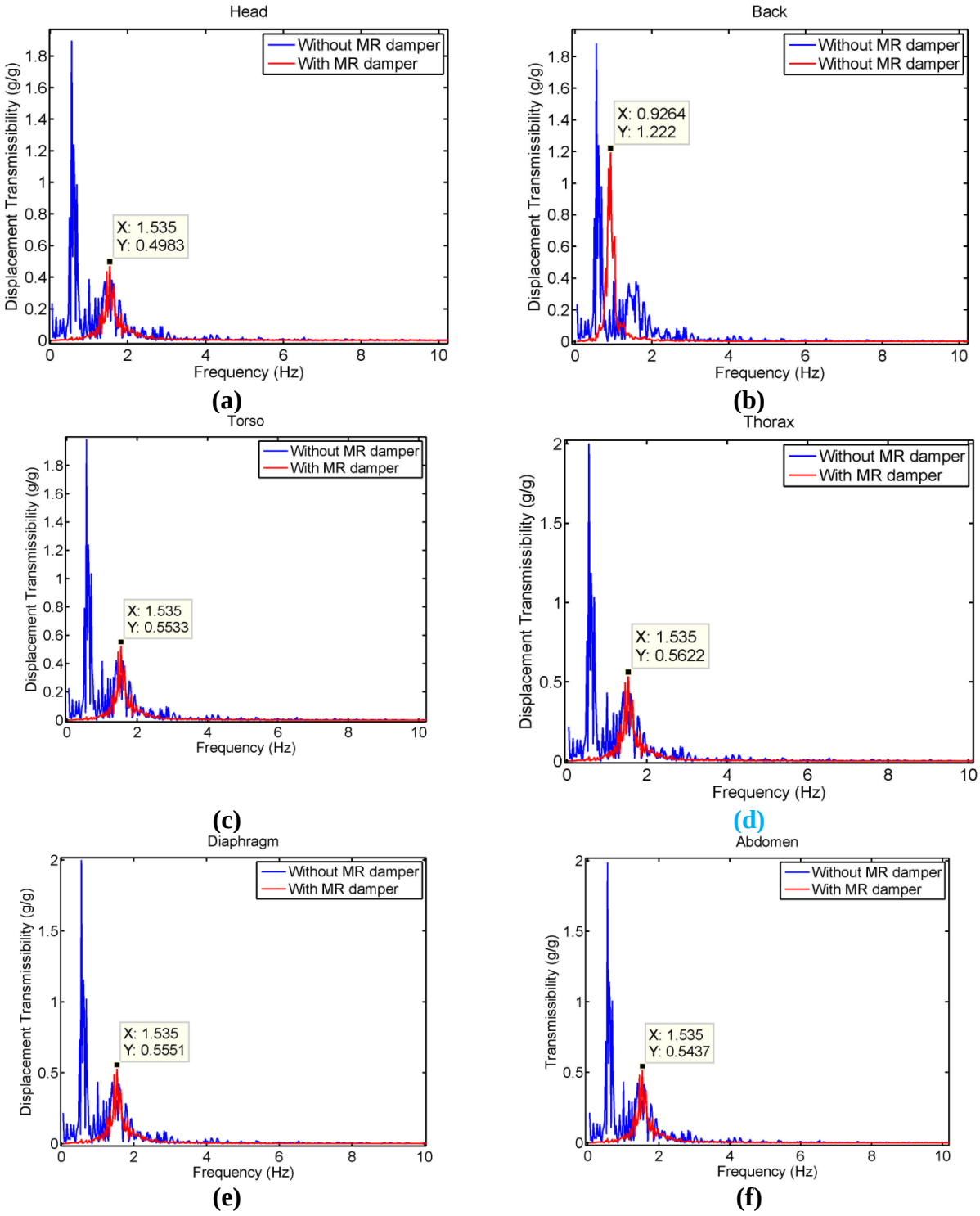

Fig.11 Typical biodynamic responses of the human body with Patil model in maneuver 1: (a) head section, (b) back section, (c) torso section, (d) thorax section, (e) diaphragm section, (f) abdomen section, (g) pelvic section.

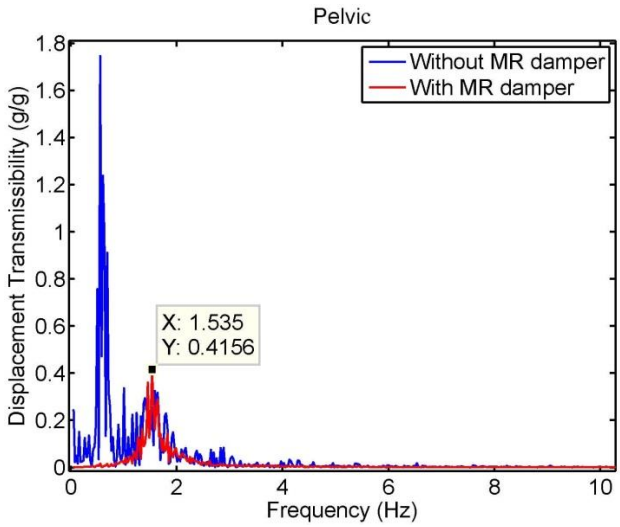

(g)

Fig.11 Typical biodynamic responses of the human body with Patil model in maneuver 1: (a) head section, (b) back section, (c) torso section, (d) thorax section, (e) diaphragm section, (f) abdomen section, (g) pelvic section.

With this model, in maneuvers 4, 5, 1, and 3, the MR damper exhibits the greatest reduction in transmissibility. However, in maneuver 2, the MR damper partly increased the transmissibility of the body organs of the pilot. The use of magnetic dampers in maneuvers 6 and 7 also shows a slight decrease in transmissibility. Referring to Figure 4, we see that the variations in acceleration versus time in maneuvers 2, 6, and 7 are small compared to other maneuvers, and it can be said that the effect of MR damper on the dynamic behavior of the system is negligible.

Table 7 Comparison of maximum transmissibility reduction

Maneuver Number	Maximum TR Wan model		Maximum TR Boileau model		Maximum TR Patil model	
	Without MR damper	With MR damper	Without MR damper	With MR damper	Without MR damper	With MR damper
5	4.45	0.18	2.6	0.23	3.95	0.27
3	3.11	0.25	1.93	0.21	1.79	0.54
4	1.88	0.36	2.4	0.4	4.18	0.58
1	2.09	0.57	0.82	0.61	2.0	0.55

To confirm the results of table 6, in this model, maneuver 1 is also selected and the biodynamic response of the pilot organs is shown in Fig. 11.

The results of Ttable 7 show that all three models showed the greatest transmissibility reduction in the use of MR damper in maneuvers 3, 4 and 5. The Wan and Patil model in maneuver 1 also shows good transmissibility reduction using MR dampers, but the Boileau model does not work well. Therefore, the Wan and Patel models are a better option. On the other hand, the Patil model gives more detailed body organs, so it can be a more complete model than the other two models.

4. Conclusion

In this paper, the effect of MR dampers on the biodynamic responses of the pilots' body has been studied in various flight maneuvers. For this purpose, discrete models of 4 and 7 degrees of freedom were used. The Bouc-Wen model was also used to model the MR damper. Differential equations of motion were obtained by Newton's method. The variations of g acceleration were recorded experimentally in different flight maneuvers and were considered as input for each of the models. Then, the biodynamical responses of the pilot's body to these inputs, without MR damper and with MR damper, were investigated. The summary of the main results obtained is as follows:

- In maneuvers where input acceleration (g variations) is large enough and changes over time, such as maneuvers 3, 4, and 5, MR damper with all three models (Wan, Boileau and Patil) has a significant effect on reducing transmissibility. On the other hand, the amount of transmissibility according to the relevant references can be directly related to the vulnerability of the body.
- In maneuvers where input acceleration is relatively large and changes over time, such as maneuver 1, MR damper with Wan and Patil models have a significant effect on reducing transmissibility, but the Boileau model does not show a good effect. So both Wan and Patil models could be better options.
- In maneuvers where input acceleration is relatively small and changes over time, such as maneuvers 2, 6, and 7, magnetic damper with the Boileau and Patil models have a weak or even negative effect on reducing conductivity, but the Wan model shows a relatively better effect. So the Wan model could be a better option.
- In general, the Patil model shows better performance in all maneuvers, so it can be a good choice for the model. On the other hand, MR dampers have a better performance in reducing transmissibility in maneuvers that have quick and abrupt input acceleration changes.

References

[1] D.F. Shanahan, G. Mastroiane, T.D. Reading, Back discomfort in US Army military helicopter aircrew member, Backache and back discomfort, (1986) 10-25.
[2] K.L. Harrer, D. Yniguez, M. Majar, D. Ellenbecker, N. Estrada, M. Geiger, Whole body vibration exposure for MH-60s pilots, in, NAVAL MEDICAL CENTER SAN DIEGO CA, 2005.
[3] A.-G. Olabi, A. Grunwald, Design and application of magneto-rheological fluid, Materials & design, 28 (2007) 2658-2664.
[4] A.N. Kulkarni, S.R. Patil, Magneto-Rheological (MR) and Electro-Rheological (ER) Fluid Damper: A Review Parametric Study of Fluid Behavior.
[5] M. Lita, N.C. Popa, C. Velescu, L.N. Vekas, Investigations of a magnetorheological fluid damper, IEEE Transactions on Magnetics, 40 (2004) 469-472.

[6] D.H. Wang, W.H. Liao, Modeling and control of magnetorheological fluid dampers using neural networks, Smart materials and structures, 14 (2004) 111.
[7] J.D. Carlson, Implementation of semi-active control using magneto-rheological fluids, IFAC Proceedings Volumes, 33 (2000) 905-910.
[8] M. Orečný, Š. Segľa, R. Huňady, Ž. Ferková, Application of a magneto-rheological damper and a dynamic absorber for a suspension of a working machine seat, Procedia Engineering, 96 (2014) 338-344.
[9] S.-B. Choi, M.-H. Nam, B.-K. Lee, Vibration control of a MR seat damper for commercial vehicles, Journal of Intelligent Material Systems and Structures, 11 (2000) 936-944.
[10] Y.-T. Choi, N.M. Wereley, Biodynamic response mitigation to shock loads using magnetorheological helicopter crew seat suspensions, Journal of aircraft, 42 (2005) 1288-1295.
[11] G.J. Hiemenz, W. Hu, N.M. Wereley, Semi-active magnetorheological helicopter crew seat suspension for vibration isolation, Journal of Aircraft, 45 (2008) 945-953.
[12] S. Kitazaki, M.J. Griffin, A modal analysis of whole-body vertical vibration, using a finite element model of the human body, Journal of Sound and Vibration, 200 (1997) 83-103.
[13] N.J. Mansfield, Human response to vibration, CRC press, 2004.
[14] Y. Matsumoto, M.J. Griffin, Modelling the dynamic mechanisms associated with the principal resonance of the seated human body, Clinical Biomechanics, 16 (2001) S31-S44.
[15] L.A. Wood, C.W. Suggs, C.F. Abrams Jr, Hand-arm vibration part III: A distributed parameter dynamic model of the human hand-arm system, Journal of Sound and Vibration, 57 (1978) 157-169.
[16] C.M. Harris, A.G. Piersol, Harris' shock and vibration handbook, McGraw-Hill New York, 2002.
[17] T.E. Coe, J.T. Xing, R.A. Shenoi, D. Taunton, A simplified 3-D human body–seat interaction model and its applications to the vibration isolation design of high-speed marine craft, Ocean engineering, 36 (2009) 732-746.
[18] M.R. Sirouspour, S.E. Salcudean, Suppressing operator-induced oscillations in manual control systems with movable bases, IEEE Transactions on Control Systems Technology, 11 (2003) 448-459.
[19] M.K. Patil, M.S. Palanichamy, A mathematical model of tractor-occupant system with a new seat suspension for minimization of vibration response, Applied Mathematical Modelling, 12 (1988) 63-71.
[20] W. Abbas, O.B. Abouelatta, M. El-Azab, M. Elsaidy, A.A. Megahed, Optimization of biodynamic seated human models using genetic algorithms, Engineering, 2 (2010) 710.
[21] N. Wilson, N. Wereley, Analysis of a magnetorheological fluid damper incorporating temperature dependence, in: 51st AIAA/ASME/ASCE/AHS/ASC Structures, Structural Dynamics, and Materials Conference 18th AIAA/ASME/AHS Adaptive Structures Conference 12th, 2010, pp. 2993.
[22] M. Braz-César, R. Barros, Experimental behaviour and numerical analysis of MR dampers, 15WCEE-15th World Conference on Earthquake Engineering, in, Portugal, 2012.
[23] A. Martins, A. Fereidooni, A. Suleman, V.K. Wickramasinghe, Test rig development and characterization of magnetorheological elastomers, in: 25th AIAA/AHS Adaptive Structures Conference, 2017, pp. 0733.
[24] R.L. Shaw, Fighter combat: tactics and maneuvers, in, Annapolis, Maryland: Naval Institute Press, 1988.